Thermochimica Acta 509 (2010) 81–86

Contents lists available at ScienceDirect

Thermochimica Acta

journal homepage: www.elsevier.com/locate/tca

Metal chloride-doped ammonia borane thermolysis: Positive effect on induction period as well as hydrogen and borazine release

R. Benzouaa, U.B. Demirci*, R. Chiriac, F. Toche, P. Miele

Université Lyon 1, CNRS, UMR 5615, Laboratoire des Multimatériaux et Interfaces, 43 boulevard du 11 Novembre 1918, F-69622 Villeurbanne, France

ARTICLE INFO

Article history:
Received 30 April 2010
Received in revised form 3 June 2010
Accepted 5 June 2010
Available online 15 June 2010

Keywords:
Ammonia borane
Chlorides
Differential scanning calorimetry
Thermogravimetric analysis
Hydrogen release by thermolysis

ABSTRACT

In this work we studied the effect of metal chlorides ($CoCl_2$, $FeCl_3$ and $AlCl_3$) on thermal decomposition of ammonia borane NH_3BH_3 (AB). The chlorides were chosen because they are simple and cost-effective. They showed promising performances as the onset temperature of AB decomposition decreased. Temperatures of 52, 65 and 85 °C were determined for $CoCl_2$-, $FeCl_3$- and $AlCl_3$-doped AB whereas it was 99 °C for AB. The induction period of AB dehydrogenation has been reduced. The relative mass losses were found as being 11.9, 12.3 and 10.4 wt% at about 110 °C but at 85 °C they were 4.5, 4.5 and 1.6 wt%, respectively. The gaseous side-products were analyzed and traces of borazine $B_3N_3H_6$ were detected. It was found that the $CoCl_2$ presence has a positive effect on the $B_3N_3H_6$ evolution. The solid by-products were characterized by XRD and IR: $[NH_2BH_2]_x$ forms after the first decomposition of AB and $[BNH_x]_z$ forms after the second decomposition. The IR-print of $[BNH_x]_z$ resembles that of BN, what suggests high dehydrogenation extent. These results are analyzed and discussed in the present paper.

1. Introduction

Molecular hydrogen (H_2) is often announced as being the energy carrier of our near future. The prospect of developing a hydrogen economy is very attractive but there are still many challenges to be addressed, one of them being hydrogen storage. Hydrogen storage is currently much investigated and science is on the lookout for finding storage solutions. In this context, ammonia borane (NH_3BH_3, AB) has showed its high potential owing to a gravimetric hydrogen density of 19.5 wt% [1]. The stored hydrogen can be released by thermal decomposition [2]. Nevertheless, AB has to release 11 wt% of pure H_2 at temperatures up to 85 °C as this value is the revised 2015 target set by the U.S. Department of Energy (US DOE) for on-board hydrogen storage systems [3]. Unfortunately, only one third of the total hydrogen content (i.e., 6.5 wt%) is recoverable in the temperature range 70–120 °C [4]. Actually, there are four main issues that hinder the effective implementing of AB: that is, a high H_2 release temperature, low content of hydrogen released up to 85 °C, too low H_2 generation rate, and storage irreversibility [5].

Promoting the H_2 release has therefore attracted much attention. In this regard, transition metal-promoted thermal decomposition [6,7] has been examined with AB. Jaska et al. [8] demonstrated the catalytic efficiency of a rhodium complex, i.e., $[Rh(1,5\text{-cod})(\mu\text{-Cl})]_2$, which nature is not exactly known. Denney et al. [9] have reported the rapid thermal decomposition of AB catalyzed by a homogeneous iridium pincer complex (i.e., (POCOP)Ir(H)$_2$ and POCOP = $[\eta^3$-1,3-$(OP^tBu_2)_2C_6H_3]$); for a 0.5 mol% catalyst loading in a tetrahydrofuran solution of AB it was observed that 1 equiv. H_2 released within 14 min at room temperature. De Benedetto et al. [10] successfully used a platinum salt, i.e., H_2PtCl_6, H_2 release starting at temperatures lower than 73 °C. Keaton et al. [11], Yang and Hall [12] and Zimmerman et al. [13] focused on active nickel N-heterocyclic carbene complexes; for example, an important H_2 release (>2.5 equiv. H_2) for a 25 wt% AB solution in diglyme was observed at 60 °C [11]. Each of the promoters given heretofore permitted to decrease the temperature of H_2 release. It is noteworthy that most of them are metal-based complexes which preparation needs more or less complicated processes and various chemicals.

In the present work, we studied the effect of metal chlorides (cobalt chloride, iron chloride and, for the first time, aluminum chloride) on thermal decomposition of AB. The reaction was considered in homogeneous solid–solid phases. Our objective was to search for simple, cost-effective, efficient metal-based activators both to reduce the induction period of AB dehydrogenation and increase H_2 release at temperatures up to 85 °C. The study was mostly based on thermogravimetric and calorimetric techniques, which can besides be coupled to gas chromatography–mass spectrometry in order to analyze the gas stream (especially the side-products). Herein, it is showed that in the presence of some of the metal chlorides we regarded the onset temperature of AB

* Corresponding author. Tel.: +33 3 72 44 84 03.
E-mail address: umit.demirci@univ-lyon1.fr (U.B. Demirci).

0040-6031/$ – see front matter © 2010 Elsevier B.V. All rights reserved.
doi:10.1016/j.tca.2010.06.007

decomposition is decreased, H_2 starting to release at temperatures much lower than 100 °C. As a matter of fact, the halides presence has a positive effect on reducing the induction period of AB decomposition as well as on decreasing the amount of unwanted gaseous side-products.

2. Experimental

AB (Sigma Aldrich, 97%), $CoCl_2$ (Acros Organics), $FeCl_3$ (Fluka) and $AlCl_3$ (Fluka) were used as received and were handled in an argon-filled glove box. Safety information: $AlCl_3$ is particularly unstable in the presence of moisture, reacting violently with generation of fumes and heat. Promoted AB samples were prepared as follows. AB and 10 wt% of metal chloride were mixed together and ground in a mortar. Reproducible results in terms of thermal and calorimetric characterizations have been obtained.

Thermogravimetric analysis (TGA) and differential scanning calorimetry (DSC) measurements were performed with TGA/SDTA 851^e and DSC1 (Mettler Toledo) under the following conditions: sample mass 2–3 mg, aluminum crucible of 100 μl with a pinhole, heating rate of 1, 3 or 5 °C min^{-1}, and atmosphere of N_2 (50 ml min^{-1}). Sample mass loss and associated thermal effects were obtained by TGA/SDTA. In order to integrate the different mass loss steps the TGA first derivation (mass loss rate) was used because even at the rate of 1 °C min^{-1} the resolution (i.e., mass loss steps well defined) was not ideal. The thermal study of the decomposition process was also investigated by DSC. Both instruments were calibrated in the studied range of temperature, i.e., 25–200 °C min^{-1}. The melting points and melting enthalpies of four standards (gallium, naphthalene, indium and tin) were used for the calibration of the DSC in terms of heat flow, temperature and tau lag. The calibration gave a straight line with a regression coefficient of 0.9997. Concerning the TGA, the melting points of five compounds (phenyl salycilate, naphthalene, benzoic acid, indium and tin) obtained from the DTA signals were used for the sample temperature calibration. The calibration gave a straight line with a regression coefficient of 1. Calcium oxalate monohydrate was used for the sample mass calibration and in doing so the experiment showed a difference in the 1st mass loss of 3.5% in relation to the theoretical value (experimental conditions: 2–3 mg of sample, heating rate of 1 °C min^{-1}, temperature range 25–200 °C). As reported by Wendlandt and co-authors [2], the AB samples undergo a voluminous swelling, which may cause an artifact on the TGA profile or a contact with the internal walls of the TGA furnace. Hence, the mass was limited to 2–3 mg (±0.01 mg). Each TGA or DSC experiment was performed three times to ensure the reproducibility of the results.

The gas stream (H_2 and side-products) was analyzed with a portable micro-chromatograph μGC M200 from Agilent M Series, which has 2 columns and 1 micro-thermal conductivity detector (μ-TCD). H_2 was separated on a molecular sieve column (12 m × 0.32 mm, 5 Å) and quantified with the TCD detector. Another OV1 column (10 m × 0.15 mm i.d.) separated borazine, its identification being realized by coupling the μGC with a mass selective detector (MSD). The μGC/MSD is commercialized by S.R.A. Instruments. As the M200 chromatograph does not permit any temperature program, preliminary measurements were undertaken to set the optimal temperature. Different column temperatures were tested: i.e., 70, 90 and 110 °C. For the present study, 90 °C was found to be the most appropriate temperature. The μGC sampling time was 20 s and the injection time 250 ms; the head column pressure was fixed at 27.8 psi for the molecular sieve column and 30.8 psi for the OV1 one. Helium and argon were used as carrier gas for the separation of borazine and H_2, respectively. Accordingly, for our sample, 2 analyses had to be done in order to separate the gases.

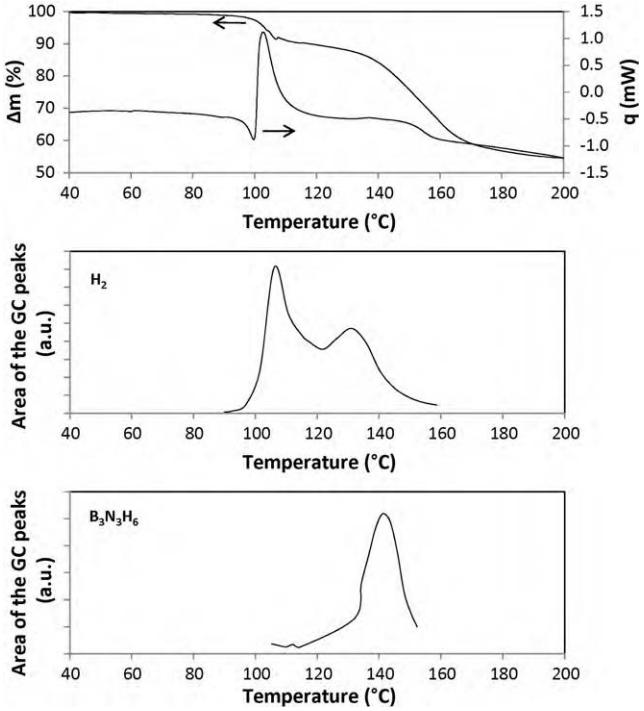

Fig. 1. TGA and DSC curves of neat AB thermolysis at a heating rate of 1 °C min^{-1} (note that the artifact on the TGA curve of neat AB at about 110 °C is due to the sample swelling [Sit-1987]) and, evolution of H_2 and that of $B_3N_3H_6$ (i.e., variation of their peak surface areas as a function of temperature; it is noteworthy that the proportion of H_2 is independent on that of $B_3N_3H_6$).

The solid by-products were recovered and analyzed by X-ray diffraction (XRD, Bruker D5005 powder diffractometer, CuKα radiation (λ = 1.5406 Å)) and diffuse reflectance Fourier transform infrared spectroscopy (IR, FTIR Nicolet 380). They were obtained in large amounts by heating 300 mg of AB (or doped AB) in a furnace at 115 °C or 200 °C (ramp 1 °C min^{-1}) under nitrogen flow (100 ml min^{-1}). No heating at 200 °C was performed on $AlCl_3$-doped AB because of the low melting point of anhydrous $AlCl_3$ (i.e., 192 °C). AB, doped AB and their by-products were handled under argon.

3. Results and discussion

3.1. Neat AB

The thermal decomposition of neat AB was first studied in our experimental conditions, which was essential to determine the best TGA/DSC operating conditions. The TGA results are summarized in Table 1. Both onset temperature and mass loss increase while the heating rate goes up. Accordingly, the heating rate of 1 °C min^{-1} was set for our experiments. The TGA curve obtained at this rate is given in Fig. 1. The thermal decomposition of AB was besides followed by DSC (1 °C min^{-1}) and showed two exothermic processes [14], i.e., two decomposition steps (99 and 132 °C), which confirmed the TGA results. The enthalpy of the first decomposition has been determined as being −16.6 kJ mol^{-1} AB (the enthalpy of the second decomposition is −7.4 kJ mol^{-1} AB). The former value has been underestimated because an endothermic peak starting at 97 °C partially compensated the first exothermic peak. Nevertheless, the apparent value is quite consistent with previously reported enthalpies from −15 to −24 kJ mol^{-1} AB [15,16]. The endothermic process is assigned to AB melting [16] which enthalpy is 2.2 kJ mol^{-1} AB.

Table 1
Thermal decomposition of neat AB and metal salt-doped AB: onset temperatures and mass losses.

Heating rate (°C min^{-1})		1	3	5
AB	*First decomposition*			
	Onset temperature (°C)	99	104	106
	Mass loss (%)	7.2	11.5	23
AB	*Second decomposition*			
	Onset temperature (°C)	132	128	139
	Mass loss (%)	35	38	46.7
AB	*First + second decomposition*			
	Mass loss (%)	42.2	49.5	69.7
Heating rate of 1 °C min^{-1}		**$CoCl_2$-AB**	**$FeCl_3$-AB**	**$AlCl_3$-AB**
Doped	*First decomposition*			
	Onset temperature (°C)	52	65	85
	Mass loss (%)[a]	10.7/11.9	11.1/12.3	9.4/10.4
Doped	*Second decomposition*			
	Onset temperature (°C)	126	132	135
	Mass loss (%)[a]	11.7/13.0	16.9/18.8	n.d.[b]
Doped	*First + second decomposition*			
	Mass loss (%)[a]	22.4/24.9	28/31.1	n.d.[b]

[a] Absolute mass loss and relative mass loss separated by "/".
[b] Not done.

The evolving gas streams were analyzed by GC–MS. Borazine ($B_3N_3H_6$) was detected whereas releases of $B_3N_3H_6$, diborane (B_2H_6) and monomeric aminoborane (NH_2BH_2) have been reported elsewhere [2,4,14–16]. Several samplings were done in the course of the AB decomposition. Fig. 1 depicts the H_2 and $B_3N_3H_6$ evolutions. The H_2 evolution started at 90 °C with 1% of total H_2 released at 95 °C. During the first decomposition (up to 120 °C), most of H_2 evolved (60% of total H_2) while ~7% of total $B_3N_3H_6$ released. In other words, $B_3N_3H_6$ mainly evolves at the second decomposition (>120 °C). In Ref. [4], the release of $B_3N_3H_6$ has for instance been reported as occurring above 127 °C. The discrepancy may be ascribed to a difference in heating rate (i.e., 5 °C min^{-1}) or in analysis detection limit.

AB and its decomposition solid by-products were analyzed by XRD and IR. From the XRD analysis (not given), it stood out that (i) the structure of AB (ICDD 01-074-0894) is confirmed, (ii) the complete decomposition of AB after the first exothermic process is observed [16], and (iii) the by-products are non-crystalline [14]. The formations of amorphous polyaminoborane $[NH_2BH_2]_x$ and polyiminoborane $[NHBH]_x$ occur at the 1st and 2nd decompositions, respectively [4]:

$$xNH_3BH_3(s) \rightarrow xNH_3BH_3(l) \quad (1)$$

$$xNH_3BH_3(l) \rightarrow [NH_2BH_2]_x(s) + xH_2(g) \quad (2)$$

$$[NH_2BH_2]_x(s) \rightarrow [NHBH]_x(s) + xH_2(g) \quad (3)$$

$$[NHBH]_x(s) \rightarrow [NB]_x(s) + xH_2(g) \quad (4)$$

The IR results (Electronic Supplementary Material ESM Fig. 1) confirmed the structure of AB [15], the formation of $[NH_2BH_2]_x$ [17] and that of $[NHBH]_x$ [15].

3.2. Doped AB

AB decomposition is described by an induction, nucleation and growth mechanistic pathway [18]. The induction period yields diammoniate of diborane $[(NH_3)_2BH_2]^+[BH_4]^-$ a reactive intermediate that is caused by disruption of dihydrogen bonds. The longer this critical period is, the higher the onset temperature of AB decomposition. Reducing it is crucial. Promoting the process by means of transition metal-based compounds has particularly been proposed. For example, Graham et al. [6] suggested the utilization of $CoCl_2$, $FeCl_3$ and $NiCl_2$ among other halides and much more recently He et al. [19] showed the positive effects of $CoCl_2$ and $NiCl_2$. Hence,

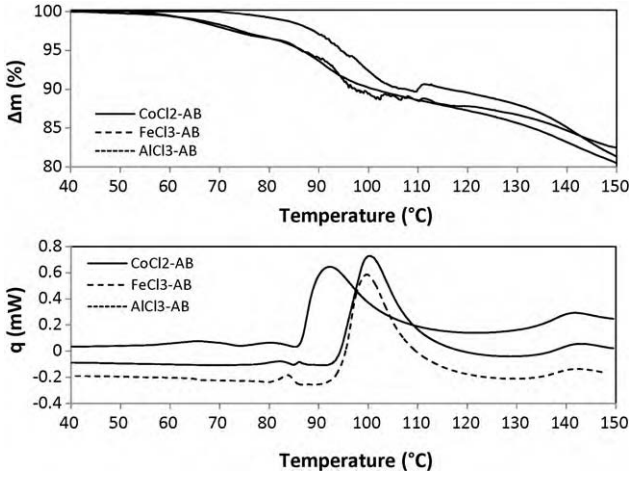

Fig. 2. TGA (top) and DSC (bottom) curves of $CoCl_2$-, $FeCl_3$-, $AlCl_3$-doped AB (heating rate: 1 °C min^{-1}).

we investigated the effect of $CoCl_2$, $FeCl_3$ and $AlCl_3$ on the thermal decomposition of AB, especially at temperatures up to 100 °C. $ZrCl_4$ and AlF_3 were also tested but the results were not convincing in our experimental conditions. AB samples doped with 10 wt% of metal chloride were prepared, the gravimetric hydrogen density being therefore dropped to 17.5 wt%.

The TGA curves are showed in Fig. 2, which main data are also reported in Table 1. It clearly appears that the onset temperature of AB decomposition is decreased in the presence of the chlorides. Temperatures of 52, 65 and 85 °C were found for $CoCl_2$, $FeCl_3$, and $AlCl_3$, respectively, whereas it was 99 °C for neat AB. $CoCl_2$ and $FeCl_3$ are as efficient as $Ni_{0.88}Pt_{0.12}$ hollow spheres [20] and $AlCl_3$ as H_2PtCl_6 [10]. Besides, our data are consistent with those in Ref. [19]; for example, a $CoCl_2$-doped AB sample started to evolve H_2 at about 50 °C. In Fig. 2, it is besides depicted that the first decomposition shows several stages [10,19]. At <120 °C, the DSC profiles show two exothermic processes for $FeCl_3$-doped AB and three for both $CoCl_2$- and $AlCl_3$-doped AB. The small decomposition peaks have all an enthalpy of −0.2 to −0.4 kJ mol^{-1} AB. The endothermic peak (AB melting) is not observed. The highly exothermic peak would very likely overlap it [10,19]. The decomposition enthalpy of the highest exothermic peak is −13.4 and −13.6 kJ mol^{-1} AB for $CoCl_2$-, $FeCl_3$-doped AB respectively, which is less exothermic than

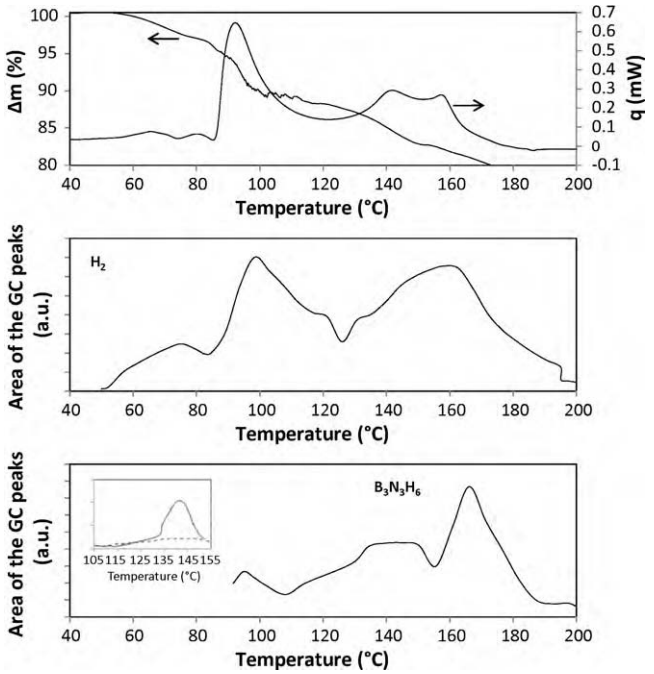

Fig. 3. TGA and DSC curves of $CoCl_2$-doped AB thermolysis at a heating rate of 1 °C min^{-1} and, proportion of H_2 and that of $B_3N_3H_6$ (i.e., variation of their peak surface areas as a function of temperature; it is noteworthy that the proportion of H_2 is independent on that of $B_3N_3H_6$); inset of the bottom figure: comparison of $B_3N_3H_6$ release from neat AB (black line) with that from $CoCl_2$-doped AB (dashed line).

the apparent decomposition enthalpy of neat AB. With regard to $AlCl_3$-doped AB, the enthalpy is −19.6 kJ mol^{-1} AB, which is higher than that of AB (i.e., −16.6 kJ mol^{-1}). Actually, the underestimation of the latter value makes any comparison difficult.

To summarize, thermal decomposition of AB can be described as follows. With respect to the $CoCl_2$-doped AB thermolysis, the 1st decomposition begins at 52 °C and shows an absolute mass loss of 10.7 wt% or a relative mass loss of 11.9 wt% [21]. Regarding the $FeCl_3$-doped sample, the 1st decomposition begins at 65 °C and shows an absolute mass loss of 11.1 wt% or a relative mass loss of 12.3 wt%. For the $AlCl_3$-doped sample, the 1st decomposition begins at 85 °C and shows an absolute mass loss of 9.4 wt% or a relative mass loss of 10.4 wt%. At 85 °C, the mass losses are 4.5, 4.5 and 1.6 wt% for $CoCl_2$-, $FeCl_3$- and $AlCl_3$-doped AB, respectively. Such values fall short of the US DOE 2015 target of (11 wt%) [3] but show that H_2 release can be promoted with simple materials. Better dehydrogenation results have been reported throughout the open literature but thermal decomposition of AB was studied in much more favorable conditions, namely in solvent [8,9,11]. Compared to both H_2PtCl_6 [10] and $Ni_{0.88}Pt_{0.12}$ hollow spheres [20], $CoCl_2$, $FeCl_3$, and $AlCl_3$ are as efficient or even more reactive. In their presence, the induction period of AB decomposition is decreased. As a result, the following classification may be suggested: $CoCl_2$ > $FeCl_3$ > $AlCl_3$.

With respect to $CoCl_2$- and $FeCl_3$-doped AB, the thermal decomposition up to 200 °C results in relative mass losses of 24.9 and 31.1 wt%, respectively. Such values are markedly lower than the mass loss of 42.2 wt% obtained with neat AB but higher than 19.5 wt% yet. As $CoCl_2$ revealed to be the best dopant in our conditions, the gas stream evolving was analyzed within the temperature range 25–200 °C. Fig. 3 shows the H_2 and $B_3N_3H_6$ evolutions with time as well the TGA and DCS profiles. In our experimental conditions, traces of $B_3N_3H_6$ were detected. He et al. [19] did not observe $B_3N_3H_6$ and this was ascribed to the fact that its concentration was beyond the detection limit of their mass spectrometer. Dehydrogenation of $CoCl_2$-doped AB is a multistep process as 3 main peaks at 71, 94 and 154 °C and 3 shoulders at 57, 121 and 132 °C are observed. Such irregular pattern indicates the formation of different solid intermediates composed of oligomeric and polymeric linear, cyclic, branched aminoboranes [19,22]. H_2 started to evolve at about 50 °C and lasted up to >200 °C whereas for neat AB the starting and ending temperatures of H_2 evolution were about 90 and 170 °C. The mol ratio [H_2 from $CoCl_2$-doped AB]/[H_2 from neat AB] were determined to be 2.2, 2.1 and 2.7 at 120, 160 and 200 °C. In other words, the dehydrogenation extent of AB in the presence of $CoCl_2$ is twice that of neat AB up to 120 °C. With respect to the mol ratio [$B_3N_3H_6$ from $CoCl_2$-doped AB]/[$B_3N_3H_6$ from neat AB], it is 0.8 and 0.3 at 120 and 160 °C. Such values imply thus that the dopant content is not enough to avoid the combination of AB molecules (isolated from $CoCl_2$) but at >120 °C the $B_3N_3H_6$ release is greatly reduced. The dopant has thus a positive effect on inhibiting the $B_3N_3H_6$ evolution. Accordingly, one may suggest that the first decomposition of AB in our experimental conditions may be called dehydrogenation.

The solid by-products obtained after the first thermal decomposition of $CoCl_2$-doped AB were analyzed by XRD and IR. The by-products were also recovered after the second thermal decomposition to be analyzed. The XRD patterns (not given) were completely similar to those of the by-products stemmed from neat AB. No peak relative to the chloride (or any metal species) was observed. After the heat treatments, the recovered solids were amorphous. The IR spectra obtained before and after the heat treatments are given in ESM Fig. 2. They are similar to those in ESM Fig. 1. The by-product obtained at 200 °C shows an IR-print like that of BN (B–N torsion at 1340–1370 and 820 cm^{-1} [15]). From both TGA and IR results as well as the data in reference [15], the formation of $[NH_2BH_2]_x$ and $[BNH_z]_x$ may be suggested. Further, it seems that the z value of $[BNH_z]_x$ tends to zero.

The solid by-products analysis was also done for $FeCl_3$- and $AlCl_3$-doped AB. The XRD patterns (not given) were similar to those of the by-products formed from neat AB. The IR spectra are given in ESM Figs. 3 and 4. Concerning the $FeCl_3$-doped AB, the striking aspect is that the relative absorbance intensities of N–H stretching (3210 cm^{-1}) and B–H stretching (about 2300 cm^{-1}) in the case of the by-product formed at 200 °C are significantly decreased, indicating a higher extent in the breaks of N–H and B–H bonds, consistently with the data in Table 1. It is also the case for the B–H torsion (1130 cm^{-1}). In other words, the IR-print is similar to the BN one, that is, to $[BNH_z]_x$ polymers, with z tending to 0. With respect to $AlCl_3$-doped AB, the thermal decomposition at 115 °C leads to the formation of $[NH_2BH_2]_x$.

4. Discussion

Strong Lewis acids are known to be initiators of AB dehydrocoupling under mild conditions [23,24] by reducing/suppressing the induction period. Heretofore, it has been showed that in the presence of $CoCl_2$, $FeCl_3$ or $AlCl_3$, the induction period can be reduced, the effect being even stronger with $CoCl_2$ and $FeCl_3$. $M^{\alpha+}$ in MCl_α acts as a Lewis site and is a site of choice for interaction with AB to form an activated complex. Dehydrocoupling between AB molecules to form new B–N bonds occurs on the $M^{\alpha+}$ surface [7] as the AB molecule is stable owing to dative bond between BH_3 and NH_3, protic NH and hydridic BH bonds, $N–H^{\delta+}\ldots^{\delta-}H–B$ dihydrogen bonds, and dipole–dipole interactions [7,25]. Accordingly, the key phenomenon that dictates AB dehydrogenation would be the network of the dihydrogen bonds between adjacent AB molecules [26]. The presence of a Lewis site $M^{\alpha+}$ may destabilize one AB molecule and, then, by chain reactions, the whole network of the dihydrogen bonds. Such a destabilization should reduce (or suppress) the induction period of AB decomposition.

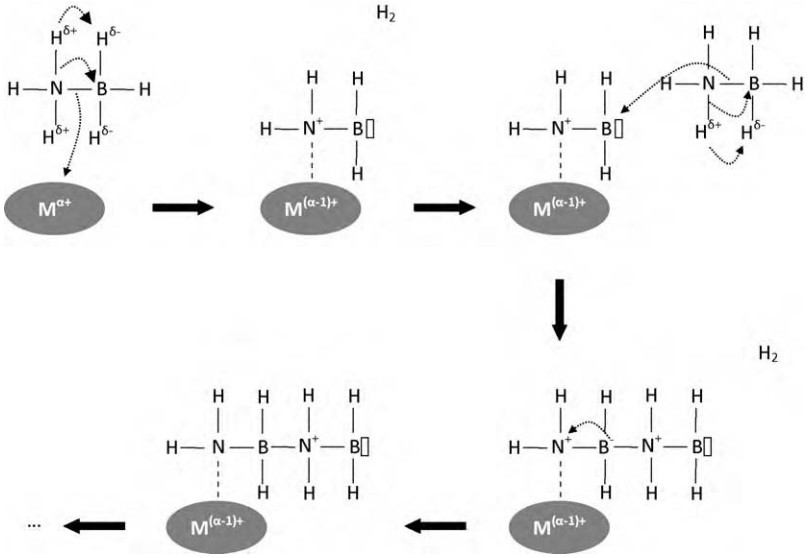

Fig. 4. Reaction of AB with $M^{\alpha+}$ of MCl_{α}.

We suggest that NH_3 of AB interacts with $M^{\alpha+}$ while H_2 is evolving (Fig. 4), resulting in the formation of $M^{(\alpha-1)+}\cdots N^{+}H_2{-}BH_2$ which lifetime is likely extremely short. Subsequent reaction with another AB then forms, leading to $M^{(\alpha-1)+}\cdots NH_2{-}BH_2{-}N^{+}H_2{-}BH_2$ with expulsion of H_2. $M^{\alpha+}$ can be seen as a polymerization catalyst and $-BH_2$ acts as a polymerization radical (cationic-like); both $M^{\alpha+}$ and $-BH_2$ are Lewis acids. Further, the M electronegativity may be a key factor for activating the first AB molecule; the more electronegative M, the more activated AB. This should result in decreasing the onset temperature, or in other words, in reducing the induction period of AB decomposition and then in accelerating AB polymerization with H_2 expulsion at each monomer addition. Our study shows that $CoCl_2 > FeCl_3 > AlCl_3$ while Co, Fe and Al have the electronegativities 1.88, 1.83 and 1.61. However, $M^{\alpha+}$ does not prevent any evolution of $B_3N_3H_6$; it however reduces it. We believe that, in places, $M^{\alpha+}$-free AB molecules start dehydrogenating and polymerizing but this is accompanied by $B_3N_3H_6$ formation by cyclization of trimers. This may be facilitated through the formation of different intermediates (oligomers, linear polymers, cyclic chains) [22], given besides that the by-products are markedly dependent on the conditions employed [17]. Accordingly, we tentatively suggest that the $M^{\alpha+}$ role is to activate the AB dehydrogenation by creating a germ, accelerating the AB polymerization and stabilizing the as-formed polymers, what reduces the $B_3N_3H_6$ emissions. Characterization of the $M^{\alpha+}$ evolution is now necessary.

5. Conclusion

Chlorides MCl_{α} are effective dopants of AB thermal decomposition. Indeed, the onset temperature is 52, 65 and 85 °C in the presence of $CoCl_2$, $FeCl_3$ and $AlCl_3$ respectively whereas it is 99 °C for neat AB. The MCl_{α} dopants permit to significantly reduce the induction period of AB decomposition. The relative mass losses are 11.9, 12.3 and 10.4 wt% at temperatures up to about 110 °C but at 85 °C, they are 4.5, 4.5 and 1.6 wt%, respectively. Such values fall short of the US DOE 2015 target (11 wt%) but show that AB dehydrogenation can be promoted with simple, inexpensive materials. Given the various types of halides, there is a wide area of investigation. The gas stream was analyzed and except H_2 the only other gas was $B_3N_3H_6$. The solid by-products were analyzed by XRD and IR. AB decomposes into $[NH_2BH_2]_x$ and then into $[BNH_z]_x$ in the presence of $CoCl_2$ or $FeCl_3$. Further, the IR-print of $[BNH_z]_x$ is like that of BN, what suggests high dehydrogenation extents and z values tending to zero. To summarize, the halides reduce the induction period of AB decomposition while they increase its decomposition extent.

Acknowledgement

Many thanks to Dr. Samuel Bernard (CNRS, CR1) for the heat treatments.

Appendix A. Supplementary data

Supplementary data associated with this article can be found, in the online version, at doi:10.1016/j.tca.2010.06.007.

References

[1] The term 'gravimetric hydrogen density' is distinguished from the term 'gravimetric hydrogen storage capacity'. The former marks out the hydrogen content of neat (or doped) AB while the latter is referred to a storage system taken as whole (including AB, dopant, tank, pipes, valves and so on).
[2] V. Sit, R.A. Geanangel, W.W. Wendlandt, Thermochim. Acta 113 (1987) 379–382.
[3] The U.S. Department of Energy 2015 target is 5.5 wt% in term of gravimetric hydrogen storage capacity. In a first approximation, we suppose that the gravimetric hydrogen storage capacity is one half of the hydrogen density, considering that the unfilled storage system weights 50% the filled one. Accordingly, the U.S. Department of Energy 2015 target is assumed to be 11.0 wt% in term of hydrogen density.
[4] F. Baitalow, J. Baumann, G. Wolf, K. Jaenicke-Rößler, G. Leitner, Thermochim. Acta 391 (2002) 159–168.
[5] U.B. Demirci, P. Miele, Energy Environ. Sci. 2 (2009) 627–637.
[6] D.R. Graham, J. Xu, G.A. Meski, United States Patent, AS 2005/0106097 A1.
[7] A. Karkamkar, C. Aardahl, T. Autrey, available at http://availabletechnologies.pnl.gov/media/87_723200830003.pdf.
[8] C.A. Jaska, K. Temple, A.J. Lough, I. Manners, J. Am. Chem. Soc. 125 (2003) 9424–9434.
[9] M.C. Denney, C.V. Pons, T.J. Hebden, D.M. Heinekey, K.I. Goldberg, J. Am. Chem. Soc. 128 (2006) 12048–12049.
[10] S.R. De Benedetto, M. Carewska, C. Cento, P. Gislon, M. Pasquali, S. Scaccia, P.P. Prosini, Thermochim. Acta 441 (2006) 184–190.
[11] R.J. Keaton, J.M. Blacquiere, R.T. Baker, J. Am. Chem. Soc. 129 (2007) 1844–1845.
[12] X. Yang, M.B. Hall, J. Am. Chem. Soc. 130 (2008) 1798–1799.
[13] P.M. Zimmerman, A. Paul, C.B. Musgrave, Inorg. Chem. 48 (2009) 5418–5433.
[14] M.G. Hu, R.A. Geanangel, W.W. Wendlandt, Thermochim. Acta 23 (1978) 249–255.
[15] J. Baumann, F. Baitalow, G. Wolf, Thermochim. Acta 430 (2005) 9–14.
[16] G. Wolf, J. Baumann, F. Baitalow, F.P. Hoffmann, Thermochim. Acta 343 (2000) 19–25.
[17] R. Komm, R.A. Geanangel, R. Liepins, Inorg. Chem. 22 (1983) 1684–1686.

[18] A.C. Stowe, W.S. Shaw, J.C. Linehan, B. Schmid, T. Autrey, Phys. Chem. Chem. Phys. 9 (2007) 1831–1836.
[19] T. He, Z. Xiong, G. Wu, H. Chu, C. Wu, T. Zhang, P. Chen, Chem. Mater. 21 (2009) 2315–2318.
[20] F. Cheng, H. Ma, Y. Li, J. Chen, Inorg. Chem. 46 (2007) 788–794.
[21] An 'absolute mass loss' is defined as being the mass loss achieved with the system MCl_α-AB (namely, the mass loss given by TGA). A 'relative mass loss' is defined as being the mass loss of AB, the mass of MCl_α being subtracted.
[22] M.E. Bluhm, M.G. Bradley, R. Butterick III, U. Kusari, L.G. Sneddon, J. Am. Chem. Soc. 128 (2006) 3578–3579.
[23] D.J. Heldebrant, A. Karkamkar, N.J. Hess, M. Bowden, S. Rassat, F. Zheng, K. Rappe, T. Autrey, Chem. Mater. 20 (2008) 5332–5336.
[24] F.H. Stephens, R.T. Baker, M.H. Matus, D.J. Grant, D.A. Dixon, Angew. Chem. Int. Ed. 46 (2007) 746–749.
[25] M.E. Bowden, G.J. Gainsford, W.T. Robinson, Aust. J. Chem. 60 (2007) 149–153.
[26] G.N. Patwari, J. Phys. Chem. A 109 (2005) 2035–2038.